Quantum Electron Transport through Ultrathin Si Films: Effects of Interface Passivation on Fermi-Level Pinning

Y. Gohda,[1,*] S. Watanabe,[2] and A. Groß[1]

[1]*Institut für Theoretische Chemie, Universität Ulm, D-89069 Ulm, Germany*
[2]*Department of Materials Engineering, The University of Tokyo, Tokyo 113-8656, Japan*
(Received 21 December 2007; revised manuscript received 14 July 2008; published 14 October 2008)

We report first-principles calculations on electron transport through ultrathin silicon films between aluminum electrodes. The passivation of interface Si atoms at one side of the film with hydrogen makes the current-voltage characteristics asymmetric with quasirectifying properties. The low conductivity in this case can be explained by the weakened metal-induced gap states due to the passivation. We also demonstrate that the applied bias changes the strength of Fermi-level pinning for the passivated interface.

DOI: 10.1103/PhysRevLett.101.166801 PACS numbers: 73.40.Sx, 73.63.Bd, 73.40.Cg

Quantum electron transport through metal-semiconductor interfaces is of strong current interest because of the miniaturization of devices both in semiconductor technology as well as in molecular electronics [1]. One of crucial factors that govern the quantum transport is the position of the Fermi level with respect to the local semiconductor band gap, i.e., the height of the Schottky-barrier forming at the metal-semiconductor interface. Experimentally, for narrow-gap semiconductors the Schottky-barrier height has been observed to be almost independent of the metal used. In order to explain this Fermi-level pinning (FLP), metal-induced gap states (MIGS) have been invoked [2–4].

MIGS are related to the evanescent states, i.e., the tails of metal states penetrating into the semiconductor, as first shown by first-principles calculations [2,3]. If the metal density of states does not vary significantly across the band gap, the distribution of MIGS is only a consequence of intrinsic features of the bulk semiconductor [4]. Thus FLP results when MIGS-induced metallic screening dominates the charge rearrangement at the interface involved with the alignment of the Fermi level. Such a role of MIGS in FLP has been demonstrated experimentally for narrow-gap semiconductors such as GaAs [5]. On the other hand, no FLP has been obtained for wide-gap semiconductors such as GaN as well as for insulators [6–8]. This is because the penetration of MIGS into the semiconductor or insulator is strongly reduced owing to the stronger decay of evanescent states.

Si is a typical semiconductor showing FLP with Schottky-barrier heights of about 0.6–0.8 eV [3,4]. However, when the interface between Al and Si(100) is passivated by a monolayer of selenium, a low Schottky-barrier height of 0.08 eV is observed [9], suggesting that FLP is suppressed and consequently that MIGS play a less dominant role in determining the interface properties between metal and Si(100). It is known that the passivation of Si dangling bonds at the Al/Si interfaces weakens the interaction between Al and Si [10]. Still, passivation does not change the intrinsic electronic structure of Si and thus should have no influence on the properties of MIGS. Thus there is an inconsistency between experimental results and the accepted view of MIGS which calls for a detailed theoretical investigation.

Furthermore, although quantum transport through nanoscale metal-semiconductor structure has been examined [11–13] in the context of the ongoing miniaturization [14,15], to the best of our knowledge there has been no theoretical investigation on the bias dependence of MIGS and FLP at metal-Si interfaces. Such bias effects are of significant importance, because changes in MIGS and the strength of FLP should strongly affect the potential distribution in the nonequilibrium region of quantum electron transport.

In this Letter, we report current-voltage (I-V) characteristics of ultrathin Si films sandwiched by Al electrodes analyzed by first-principles transport calculations based on density functional theory [16,17]. Whereas the ideal Al-Si-Al contact exhibits conducting behavior due to the presence of MIGS, the passivation of the Si dangling bonds at one side of the film by hydrogen suppresses the MIGS considerably and changes the I-V characteristics drastically resulting in diodelike behavior. This finding resolves the inconsistency between theory and experiments. Furthermore, we demonstrate that the strength of FLP is dependent on the applied bias for the H-passivated Si-Al interface resulting in an asymmetric I-V curve. The present results clarify the importance of controlling interface structures on the atomic scale.

The current was calculated by the boundary-matching scattering-state density functional (BSDF) method [18–20] within the local density approximation [21,22] incorporating explicitly current-carrying states, semi-infinite electrodes, and effects of the applied bias voltage. We employed local pseudopotentials for the ionic cores of the atoms [23–26]. The Si local pseudopotential has been used in previous transport calculations [11], which reproduces the magnitude of the Si band gap (1.2 eV) appropri-

 © 2008 The American Physical Society

ately and the band structure satisfactorily [23]. This feature is of merit since empty states enter in the transport window for finite biases [27], although this potential could introduce small errors other than the band gap far from the Fermi level as a trade-off. The bias voltage is defined relative to the left electrode, which means that the one-electron effective potential of the right electrode drops for positive bias voltages.

A ten-layer Si(100) slab with the thickness of approximately 1.4 nm was sandwiched by Al(100) electrodes that were modeled by two-layer Al slabs attached to semi-infinite jellium. The Al(100) slabs are compressed to form an Al(100)-Si(100) interface avoiding the lattice mismatch of ~5%. Since it has been pointed out that doping is not favorable for ultrathin Si films [12,28], no dopants were included in our models. We calculated the unpassivated Al-Si(100) interface as well as the one where Si atoms at the right side of the slab are passivated by hydrogen using the canted 1×1 dihydride phase [29,30]. The atomic structures of Si and H atoms for the zero-bias case were optimized by using the VASP code [31], while we fixed Al atoms at the bulk positions. We have found that the outermost silicon atoms of the unpassivated interface prefer the hollow site of Al(100) forming chemical bonds [Fig. 1(b)], whereas the hydrogen atoms for the H-terminated interface are located at the top site interacting only weakly with the Al atoms [Fig. 1(c)]. Note that also in the 2×1 monohydride phase there is only 1 H atom in direct contact with the Al atoms at the interface, but again weakly interacting with Al so that the electronic interactions are rather similar to the 1×1 H-passivated interface. We also considered the possibility of the Si 2×1 reconstruction for the unpassivated interfaces. Silicon forms direct chemical bonds with the Al atoms at the interface which makes the 2×1 dimerization unfavorable by 0.2 eV per 1×1 interface unit cell. Therefore, we used the 1×1 structure also for the unpassivated interface in our calculations. The 1×1 atomic configurations adopted in the BSDF calculations were kept frozen during the application of the bias. The grid spacing in the real-space discretization for the direction perpendicular to the interface is set to be 0.15 Å, and the lateral cut-off energy is set to be 6 Ry.

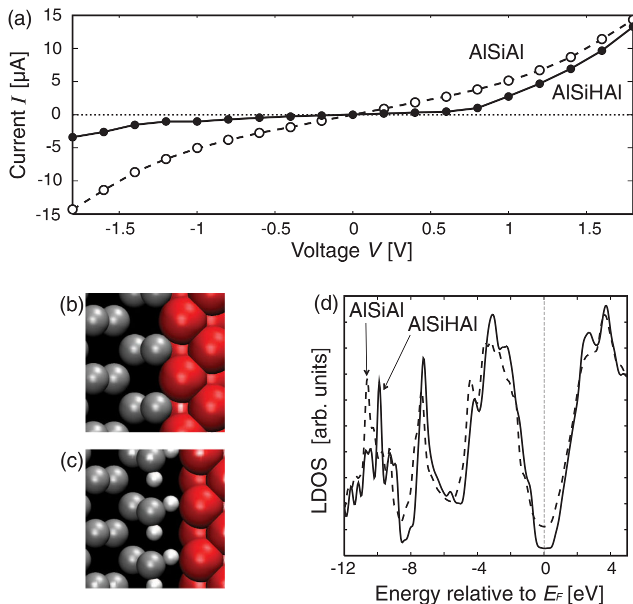

FIG. 1 (color online). (a) Calculated I-V characteristics of ultrathin Si films. The values of the current is per Si atoms at the interface. (b) Atomic structure of the unpassivated interface between the Si film and the right Al electrode. (c) Atomic structure of the H-passivated interface. The interface between the Si film and the left Al electrode is unpassivated for both cases of AlSiAl and AlSiHAl. (d) Local density of states for the region between third and fourth Si atoms from the right side of the thin films in the zero-bias case [Region II in Fig. 2(a)]. Empty states are also shown in this figure.

As Fig. 1(a) shows, the calculated I-V characteristics of ultrathin Si films at small biases is essentially linear for the ultrathin film with the unpassivated interfaces (AlSiAl, dashed line). This linearity comes from a metallization due to the presence of MIGS. Since the electron transport does not occur through Si chemical bonds but through MIGS, the zero-bias conductance per Si atoms at the interface of approximately 0.05 G_0 is considerably smaller than the conductance quantum $G_0 = 2e^2/h$.

On the other hand, the I-V characteristic is asymmetric for the film with the Si atoms at the right interface passivated by H (AlSiHAl, solid line). For negative biases, the current is rather small, indicative of rectifyinglike behavior. For positive biases, the current approaches to that of AlSiAl as the bias increases, although the magnitude of the current is smaller than for AlSiAl at all biases examined. The zero-bias conductance per Si atoms at the interface is approximately 0.008 G_0.

As a first step to clarify the considerable difference in the I-V characteristics for AlSiHAl and AlSiAl, we have calculated the local density of states (LDOS) as shown in Fig. 1(d). As clearly seen in the vicinity of the Fermi level, the LDOS associated with the MIGS of AlSiHAl is much smaller than that of AlSiAl. This explains the fact that the current of AlSiHAl in the low bias regime is significantly smaller than that of Al-Si-Al (Fig. 1). This fact solves the controversy mentioned above, because it is consistent with both the previous theoretical studies that showed FLP for the unpassivated interface due to MIGS [2–4] and the experiment finding an absence of the pinning induced by the passivation [9], which can now be interpreted as caused by the reduced density of MIGS. It should be pointed out that, although it has often been interpreted as if MIGS are independent of the interface atomic structure [9], the amplitude of MIGS can depend on the condition of the interface even though MIGS are a consequence of intrinsic bulk properties. The present result demonstrates clearly that the amplitude of MIGS is controllable by the passivation.

Next, we have analyzed the dependence of the effective potential on the applied bias, because the *I-V* characteristics for large biases for AlSiHAl cannot be explained from the LDOS for the zero-bias case [Fig. 1(d)]. Figure 2(a) shows the effective potential of AlSiHAl for $V = 0$ and its shifts with respect to $V = 0$ for $V = 1.8$ and -1.8 V that are chosen as samples of positive and negative voltages reasonably far from zero. The asymptotic values of the potential shifts that are calculated as the difference in the effective potential correspond to $-V$ in the right electrode. The potential at the right interface with passivation is much higher than that at the unpassivated Al-Si interface on the left-hand side. This high potential plays the role of a barrier; it suppresses the penetration of the MIGS into the semiconductor and thus reduces the density of the gap states, as seen in Fig. 1(d). It is attributed to the fact that the chemical interaction between Al and Si is weak because of the H termination for the passivated interface resulting in the concentration of the potential change due to the applied bias at the right interface region. A concentration of the potential change has also been found for Ag-Ag_2S-Ag interface structures [32] as well as atomic chains [33]. However, surprisingly, the fashion of the potential-drop concentration depends strongly on the applied bias: For $V = 1.8$ V, it is clear that the potential drop concentrates entirely at the passivated interface while there is almost no shift in the Si thin film; in contrast, the potential change due to the applied bias is also seen inside of Si for $V = -1.8$ V.

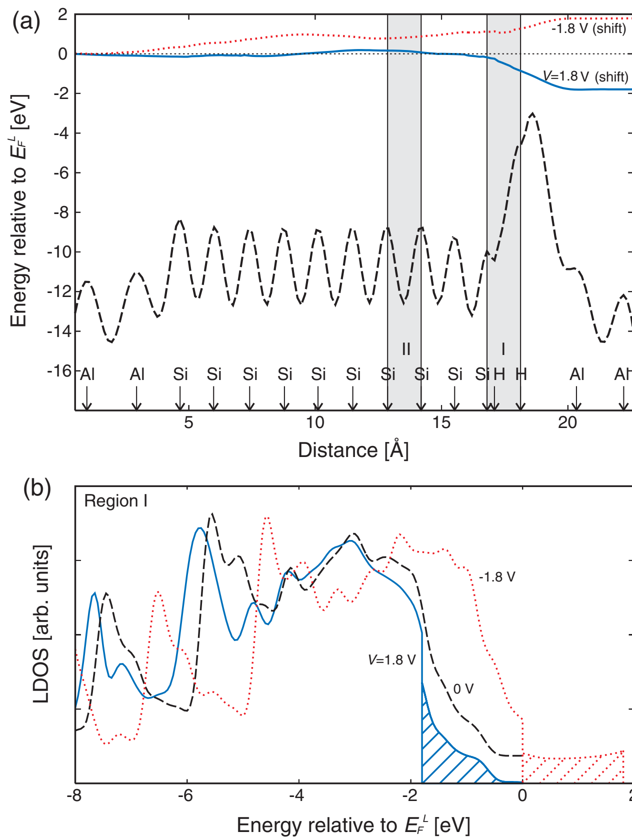

FIG. 2 (color online). (a) Effective potential of AlSiHAl for $V = 0$ (dashed line) and its shifts due to applied biases of $V = 1.8$ (solid line) and -1.8 V (dotted line). (b) Local density of states for the region between the Si atom at the passivated interface and the outermost H atom of AlSiHAl [Region I in (a)]. The hatched LDOS represents nonequilibrium states in the transport window.

The concentration of the potential shift for $V = 1.8$ V shown in Fig. 2(a) implies that the potential shift at the interface is an important clue. Figure 3 shows the shift of the potential for the Si atom at the right interfaces relative to the right electrode for AlSiHAl and AlSiAl. Since the LDOS of Si shifts according to the potential shifts without changing the general feature except for the nonequilibrium regime, i.e., inside of the transport window, as seen in Fig. 2(b), such potential shifts are helpful to clarify the essential characteristics of FLP. For AlSiAl, the potential of Si hardly changes by the applied bias voltages investigated, which agrees well with FLP obtained in the previous work [2]. On the other hand, at the passivated interface of AlSiHAl, the Si potential shifts due to the applied bias indicating that the passivation makes FLP weak, which is consistent with experiment [9]. In particular, the shift for positive biases nearly corresponds to the applied bias meaning almost perfect removal of FLP. However, for negative biases, the shift exhibits intermediate behavior due to the wide distribution of the potential drop, suggesting that the strength of FLP for the passivated interface depends on the applied bias. To understand the mechanism of this bias dependence, we will focus again on the cases of $V = 1.8$ and -1.8 V below.

For $V = 1.8$ V, the Al side of the passivated interface is positively charged due to the applied bias by -0.05 electrons per interface unit cell, which suppresses the metal-induced states. This suppression of metal-induced states reduces their penetration into the Si layer so that the potential drop can only occur at the interface but not inside of the Si film and the potential inside of the Si ultrathin film

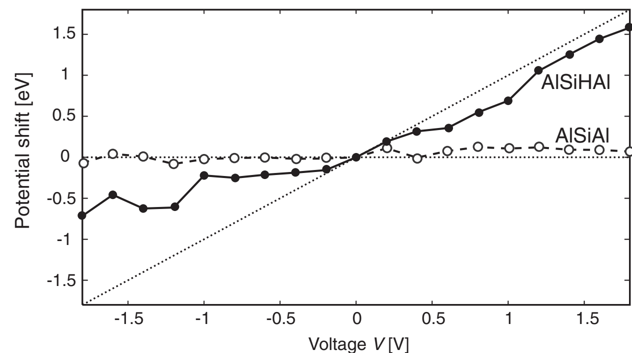

FIG. 3. Shift of the potential ΔV for the Si atom at the right interfaces relative to the right electrode. The lines for $\Delta V = 0$ and $\Delta V = V$ are also shown.

is hardly affected by the change in the chemical potential of the right Al electrode μ^R. Indeed, MIGS from the right electrode do not exist for $V = 1.8$ V, because the nonequilibrium states in the transport window seen in Fig. 2(b) consist entirely of states from the left-hand side of the interface. Because of the lack of the potential shift inside of the Si film, a considerable part of the Si valence band enters into the transport window resulting in the large amount of the current obtained. This mechanism is confirmed by calculating the current spectrum that has a remarkable peak at the right Fermi level. In contrast, the amount of occupied metal states from the right electrode including MIGS penetrating into the Si layer increases due to the applied bias for $V = -1.8$ V leading to a potential drop that becomes more delocalized.

To confirm the generality of our findings, we also investigated the passivation by selenium. We have found that the Se atom passivating the Si dangling bonds prefers the Al top site. A potential barrier similar to the one seen in the H-passivated interface is also found for the Se-passivated interface, with the height being 3.8 eV lower than the one for the H-passivated interface. This lower barrier should be attributed to the higher electronegativity of Se than H. Nevertheless, this potential barrier also induces a pronounced potential drop due to the bias voltage as seen at the H-passivated interfaces. We confirmed that the strength of FLP at the Se-passivated interface is stronger for positive biases than negative ones, i.e., exhibiting the same qualitative dependence on the bias voltage as the H-passivated interface; although the potential change is quantitatively more delocalized due to the lower potential barrier.

In conclusion, we have studied the coherent electron transport through ultrathin Si films sandwiched by Al electrodes using first-principles transport calculations. We have found that interface passivation leads to potential barriers at the interface which reduces the penetration of MIGS into the semiconductor and thus explains the suppression of FLP for passivated interfaces. However, the strength of FLP depends on the bias resulting in significant changes in the I-V characteristics.

One of the authors (Y. G.) wishes to acknowledge the support from the Alexander von Humboldt Foundation. This work has been supported by the German Science Foundation (DFG) through Contract GR 1503/18-1.

*gohda@phys.s.u-tokyo.ac.jp
Present address: Department of Physics, The University of Tokyo, Tokyo 113-0033, Japan.

[1] *Introducing Molecular Electronics*, edited by G. Cuniberti, G. Fagas, and K. Richter (Springer, Berlin, 2005).
[2] S.G. Louie and M.L. Cohen, Phys. Rev. B **13**, 2461 (1976).
[3] S.G. Louie, J.R. Chelikowsky, and M.L. Cohen, Phys. Rev. B **15**, 2154 (1977).
[4] J. Tersoff, Phys. Rev. Lett. **52**, 465 (1984).
[5] T.C.G. Reusch *et al.*, Phys. Rev. Lett. **93**, 206801 (2004).
[6] S. Picozzi *et al.*, Phys. Rev. B **61**, 16 736 (2000).
[7] J.I. Iwata, K. Shiraishi, and A. Oshiyama, Appl. Phys. Lett. **83**, 2560 (2003).
[8] M. Kiguchi *et al.*, Phys. Rev. Lett. **90**, 196803 (2003).
[9] M. Tao *et al.*, Appl. Phys. Lett. **83**, 2593 (2003).
[10] T.C. Shen, C. Wang, and J.R. Tucker, Phys. Rev. Lett. **78**, 1271 (1997).
[11] U. Landman, R.N. Barnett, A.G. Scherbakov, and Ph. Avouris, Phys. Rev. Lett. **85**, 1958 (2000).
[12] F.G. Pikus and K.K. Likharev, Appl. Phys. Lett. **71**, 3661 (1997).
[13] M. Jang *et al.*, Appl. Phys. Lett. **84**, 741 (2004).
[14] M. Lundstrom, Science **299**, 210 (2003).
[15] M. Ieong *et al.*, Science **306**, 2057 (2004).
[16] P. Hohenberg and W. Kohn, Phys. Rev. **136**, B864 (1964).
[17] W. Kohn and L.J. Sham, Phys. Rev. **140**, A1133 (1965).
[18] Y. Gohda and S. Watanabe, Phys. Rev. Lett. **87**, 177601 (2001).
[19] S. Furuya, Y. Gohda, N. Sasaki, and S. Watanabe, Jpn. J. Appl. Phys. **41**, L989 (2002).
[20] Y. Gohda and S. Watanabe, J. Phys. Condens. Matter **16**, 4685 (2004).
[21] D.M. Ceperley and B.J. Alder, Phys. Rev. Lett. **45**, 566 (1980).
[22] J.P. Perdew and A. Zunger, Phys. Rev. B **23**, 5048 (1981).
[23] M. Schlüter, J.R. Chelikowsky, S.G. Louie, and M.L. Cohen, Phys. Rev. B **12**, 4200 (1975).
[24] J.R. Chelikowsky, D.J. Chadi, and M.L. Cohen, Phys. Rev. B **23**, 4013 (1981).
[25] P. Giannozzi (unpublished).
[26] F. Gygi, Phys. Rev. B **48**, 11692 (1993).
[27] X.G. Zhang, Z.Y. Lu, and S.T. Pantelides, Appl. Phys. Lett. **89**, 032112 (2006).
[28] P. Zhang *et al.*, Nature (London) **439**, 703 (2006).
[29] S. Ciraci and I.P. Batra, Surf. Sci. **178**, 80 (1986).
[30] J.E. Northrup, Phys. Rev. B **44**, 1419 (1991).
[31] G. Kresse and J. Furthmüller, Phys. Rev. B **54**, 11 169 (1996); Comput. Mater. Sci. **6**, 15 (1996).
[32] Z. Wang, T. Kadohira, T. Tada, and S. Watanabe, Nano Lett. **7**, 2688 (2007).
[33] K. Hirose, N. Kobayashi, and M. Tsukada, Phys. Rev. B **69**, 245412 (2004).